Viability, function and morphological integrity of precision-cut liver slices during prolonged incubation

Starokozhko, Viktoriia; Abza, Getahun B; Maessen, Hedy C; Merema, Marjolijn T; Kuper, Frieke; Groothuis, Geny M M

Published in:
Toxicology in Vitro

DOI:
10.1016/j.tiv.2015.10.008

Publication date:
2015

Toxicology in Vitro 30 (2015) 288–299

Contents lists available at ScienceDirect

Toxicology in Vitro

journal homepage: www.elsevier.com/locate/tiv

Viability, function and morphological integrity of precision-cut liver slices during prolonged incubation: Effects of culture medium

Viktoriia Starokozhko [a], Getahun B. Abza [a], Hedy C. Maessen [a], Marjolijn T. Merema [a], Frieke Kuper [b], Geny M.M. Groothuis [a,*]

[a] Division of Pharmacokinetics, Toxicology and Targeting, Groningen Research Institute for Pharmacy, University of Groningen, Antonius Deusinglaan 1, 9713 AV Groningen, The Netherlands
[b] TNO, Utrechtseweg 48, 3704 HE Zeist, The Netherlands

ARTICLE INFO

Article history:
Received 10 September 2015
Received in revised form 20 October 2015
Accepted 24 October 2015
Available online 26 October 2015

Keywords:
Precision-cut liver slices
Prolonged incubation

ABSTRACT

Precision-cut liver slices (PCLS) are an ex vivo model for metabolism and toxicity studies. However, data on the maintenance of the morphological integrity of the various cell types in the slices during prolonged incubation are lacking. Therefore, our aims were to characterize morphological and functional changes in rat PCLS during five days of incubation in a rich medium, RegeneMed®, and a standard medium, Williams' Medium E. Although cells of all types in the slices remain viable, profound changes in morphology were observed, which were more prominent in RegeneMed®. Slices underwent notable fibrosis, bile duct proliferation and fat deposition. Slice thickness increased, resulting in necrotic areas, while slice diameter decreased, possibly indicating cell migration. An increased proliferation of parenchymal and non-parenchymal cells (NPCs) was observed. Glycogen, albumin and Cyp3a1 were maintained albeit to a different level in two media. In conclusion, both hepatocytes and NPCs remain viable and functional, enabling five-day toxicity studies. Tissue remodeling and formation of a new capsule-like cell lining around the slices are evident after 3–4 days. The differences in effects between media emphasize the importance of media selection and of the recognition of morphological changes in PCLS, when interpreting results from toxicological or pharmacological studies.

1. Introduction

During the drug-development process, many signs of toxicity go unnoticed due to the absence of good predictive models and specific toxicity biomarkers. As a result, liver toxicity is a major problem in drug development. Therefore, there is interest in developing reliable liver models for early detection of toxic effects of drugs. Since in vivo methods imply the use of a large number of animals, during the past decades more attention has been given to design and validate alternative models for drug toxicity testing that lead to reduction and eventually replacement of animal use. In addition to the widely used cultures of freshly isolated cells or cell lines, precision-cut liver slices (PCLS) were developed as an ex vivo model, which has already been proven to be functional and efficient in numerous metabolism and toxicity studies (de Graaf et al., 2007; Elferink et al., 2008; Hadi et al., 2012; Parrish et al., 1995). The main advantage of this model above cell lines is that all liver cell types are present in their original tissue-matrix configuration (de Graaf et al., 2007; Soldatow et al., 2013). This is a major advantage, as it is well known that also the non-parenchymal cells, such as Kupffer cells (KCs) and hepatic stellate cells (HSCs), in the liver may contribute considerably to the toxic effects of drugs. Following injury, KCs are activated by pro-inflammatory signals. They are the primary cells engaged in inflammatory responses and promote the repair and regeneration of injured tissue (Roberts et al., 2007). Activated KCs release different fibrogenic cytokines such as tumor necrosis factor alpha (TNF-α), platelet-derived growth factor (PDGF), and transforming growth factor (TGF-β) which induce the activation of HSCs leading to the synthesis and deposition of connective tissue (Zhou et al., 2014).

There is a major restriction, however, related to this model. The use of PCLS was long time limited by their relatively short viability (1–2 days), as reported in many studies (Catania et al., 2003; de Graaf et al., 2010; Goethals et al., 1990; Lerche-Langrand and Toutain, 2000). Formation of necrotic areas occurred in slices incubated beyond 48 h and metabolic activities decreased (Hashemi et al., 1999; Lerche-Langrand and Toutain, 2000; Price et al., 1998; Soldatow et al., 2013; Toutain et al., 1998). Even though several research labs managed to keep PCLS viable for more than 72 h (Catania, 2007; Martin, 2002; Vickers et al., 2004), hardly any data are available on the maintenance of the morphological integrity of the various cell types in the slices during prolonged incubation, which hamper the interpretation of the data obtained.

There are several factors, which could affect the longevity of the tissue and cell morphology, including oxygen concentration (Halliwell, 2014; Toutain et al., 1998), pH, temperature and composition of the incubation medium (Chan, 2002; Chan et al., 2003; Iyer et al., 2010).

* Corresponding author.
E-mail address: g.m.m.groothuis@rug.nl (G.M.M. Groothuis).

http://dx.doi.org/10.1016/j.tiv.2015.10.008
0887-2333/

Medium composition not only affects the viability of primary rat hepatocytes, but also has a direct effect on their functionality and sensitivity to xenobiotic exposure (Doostdar et al., 1988; Elaut et al., 2005). The majority of media intended for in vitro liver preparations are designed specifically for culturing hepatocytes and biliary epithelial cells, neglecting other non-parenchymal liver cells (NPCs). NPCs were shown to be subject to necrosis during PCLS incubation, leading to the disruption of cell heterogeneity possibly as a result of inappropriate medium composition (Toutain et al., 1998). No extensive studies have been published to our knowledge demonstrating the influence of different types of media on rat PCLS viability, cell type composition, morphology and function during prolonged incubation. Therefore, we aimed to investigate the effect of prolonged (up to 5 days) incubation in two different media on the viability of the different cell types in rat PCLS cultures. Williams' Medium E (WME) was chosen as an example of a standard cell culture medium that is commonly used for PCLS incubation, but its effects on PCLS, however, have never been fully characterized during prolonged incubation (Duryee et al., 2014; Jetten et al., 2014; Westra et al., 2014). As second medium, we selected the enriched RegeneMed® medium, which has been initially designed and used to culture primary hepatocytes together with NPCs, such as KCs, HSCs, vascular endothelial cells and bile duct epithelial cells (BECs) (Kostadinova et al., 2013). We characterized the morphological and functional changes in PCLS during five days (120 h) of incubation in these two media using standard viability tests and (immune)histochemical staining specific for hepatocytes, KCs, HSCs, BECs as well as for mesenchymal and mesothelial cells.

2. Material and methods

2.1. Animals

Male Wistar rats were obtained from Charles River (Sulzfeld, Germany). The rats were housed in a temperature- and humidity-controlled room on a 12 h light/dark cycle with food and tap water ad libitum (Harlan Laboratories B.V., Horst, The Netherlands). Animals were allowed to acclimatize for at least seven days before starting the experiments. All experiments were approved by the Animal Ethical Committee of the University of Groningen.

2.2. Excision of rat liver

Under isofluorane/O_2 anesthesia, the liver was excised and placed into the ice-cold University of Wisconsin (UW) organ preservation solution (DuPont Critical Care, Waukegab, IL) until the start of the slicing procedure.

2.3. Preparation and incubation of rat PCLS

PCLS were prepared as described previously by de Graaf et al. with minor modifications (de Graaf et al., 2010). In brief, 5 mm cylindrical cores of liver tissue were made by using a hollow drill bit. Cores were sliced with a Krumdieck tissue slicer (Alabama R&D, Munford, AL, USA), which was filled with ice-cold Krebs–Henseleit buffer supplemented with 25 mM D-glucose (Merck, Darmstadt, Germany), 25 mM $NaHCO_3$ (Merck), 10 mM Hepes (MP Biomedicals, Aurora, OH, USA) and saturated with a mixture of 95% oxygen and 5% CO_2. Rat PCLS (about 200 μm thickness and 5 mg wet weight) were stored in ice-cold UW solution until use. They were pre-incubated in the incubator (Panasonic, USA) for 1 h at 37 °C in a 12-well plate filled with 1.3 mL of WME saturated with 80%O_2/5:CO_2 while gently shaking 90 times per minute, to restore their function and remove cell debris. Thereafter, slices were transferred to another 12-well plate filled with 1.3 mL of two different types of media saturated with 80%O_2/5CO_2: WME (with L-glutamine, Invitrogen, Paisly, Scotland) supplemented with 25 mM glucose and 50 mg/mL gentamycin (Invitrogen) or RegeneMed® medium (WME supplemented with RegeneMed® additives (L3STA), antibiotics (L3MAB) and supplements (L3STS) in ratio 100:15.1:1:2.5 (RegeneMed®, San Diego, CA, USA)). Medium was refreshed daily.

2.4. ATP and protein content of PCLS

Viability of PCLS incubated in different media was determined at different time points (24, 48, 72, 96, 120 h) by means of the ATP content of the PCLS as described previously (de Graaf et al., 2010). In brief, after each experimental time point three replicate slices for each experimental group were collected individually in 1 mL of 70% (*v*/*v*) ethanol containing 2 mM EDTA (pH 10.9) and frozen immediately. Samples were stored at −80 °C until analysis. After thawing and homogenization using a Mini-BeadBeater 24 (Biospec Products, Bartlesville, USA) the samples were centrifuged at 16,100 *g* for 5 min at 4 °C. The supernatant was diluted 10 times with 0.1 M Tris HCl buffer containing 2 mM EDTA (pH 7.8) and the ATP content was determined by using the ATP Bioluminescence Assay Kit CLS II (Roche, Mannheim, Germany) in a black 96-well plate Lucyl luminometer (Anthos, Durham, NC) according to the manufacturer's protocol using a standard ATP calibration curve. The pellet of the homogenized samples was used to determine the protein content of the PCLS. Briefly, the pellet was dissolved in 200 μL of 5 M NaOH for 30 min at 37 °C. After dilution with 800 μL mQ water, the protein content was measured according to Lowry by using the Bio-Rad DC Protein Assay (Bio-Rad, Munich, Germany) using a bovine serum albumin calibration curve (Lowry et al., 1951). The absorbance was read at 650 nm after keeping a plate in the dark for 15 min.

2.5. LDH leakage

LDH leakage from the slice to the medium was used as a marker of cell damage. In brief, medium was collected after every experimental time point and stored at 4 °C until analysis. The LDH assay was performed using the Cyto Tox-ONE Homogenous Membrane Integrity Assay kit (Promega, Madison, USA) according to the manufacturer's instructions with slight modifications. Accordingly, 50 μL of medium sample was mixed with 50 μL of the substrate mix in a black 96-well plate. The reaction was allowed to continue for 10 min, after which the stop reagent was added to the mixture. Fluorescence was read at excitation 590 nm and emission 560 nm. The LDH content of the PCLS after 1 h pre-incubation was used as a 100% value of LDH content in a slice at the beginning of the incubation. For that, three slices were collected separately in a tube containing 1.3 mL of fresh medium. Slices were homogenized and samples centrifuged at 16,100 *g* for 2.5 min. Thereafter the supernatant was collected and processed in the assay together with the other samples.

2.6. Paraffin- and cryosections of PCLS

All experimental groups were subjected to morphological evaluation. For paraffin imbedding PCLS were collected after each experimental time point and fixed in 4% formaldehyde in phosphate buffered saline (PBS) solution for 24 h at 4 °C and stored until analysis in 70% ethanol at 4 °C. After dehydration in alcohol and xylene, the slices were embedded in paraffin and sectioned (sections 4 μm thick) perpendicular to the surface of the slice.

To prepare cryosections, fresh PCLS were embedded in KP-cryocompound (Klinipath, The Netherlands) and frozen in 2-methylbutane (Sigma-Aldrich, Germany) at −80 °C. Sections of 4 μm thick were prepared using a CryoStar NX70 cryostat (Thermo Fisher Scientific, Germany) perpendicular to the surface of the slice.

2.7. Morphological assessment

Morphological assessment of PCLS was performed on paraffin sections, stained with hematoxylin and eosin (Klinipath, The Netherlands) (H&E) as described previously (de Graaf et al., 2000).

2.8. Thickness scoring

The thickness of the slices was measured using the Image J program using the H&E stained paraffin sections. Five measures were taken in different areas of each individual slice and the average value was calculated per slice. The average thickness of three slices in every experimental group was calculated.

2.9. General immunostaining procedure

4 μm paraffin sections were deparaffinized and rehydrated. Antigen retrieval was performed by incubating sections in citrate buffer (10 mM, pH = 6) for 20 min at 90 °C, with the exception of desmin and albumin staining where incubation in 0.1 M Tris–HCl buffer (pH 9) overnight at 80 °C was used. Cryosections were allowed to dry for 30 min at room temperature (RT) prior to acetone (at −20 °C for 5 min) or 2% formaldehyde (at RT for 10 min) fixation. Thereafter, the first antibody was applied for 60 min at RT. The concentration of primary antibodies was optimized in pilot experiments. Endogenous peroxidase activity was inhibited by incubating the sections in 0.3% H_2O_2 (VWR, Fontenaysous-Bois, France) in methanol for 20 min. Afterwards, the secondary antibody was applied followed by the tertiary antibody (for 30 min each). The antibodies used are shown in Table 1. Normal rat serum (NRS) was added (5%) to the secondary and tertiary antibodies to block non-specific binding. Antigen–antibody complexes were visualized by staining with di-aminobenzidine (DAB) chromogen with H_2O_2 for 20 min or with ImmPact NovaRed (Vector, Burlingame, USA) for 15 min and counterstained with hematoxylin for 1 min. After the dehydration, slides were covered with a cover slip using Depex (Prolabo, Leuven, Belgium) and were examined under the microscope.

2.10. Oil Red O staining

Lipid (triglyceride) accumulation in PCLS was examined using ORO staining as described previously by *Kinkel* et al. with some modifications (Kinkel et al., 2004). In brief, cryosections were air dried and fixed with 4% formaldehyde/PBS for 10 min at room temperature. After that, the sections were immersed in 60% 2-propanol briefly two times and then stained in ORO solution (0.6 mg ORO powder in 36% 2-propanol) for 10 min. Thereafter, the slides were again briefly dipped in 60% 2-propanol and rinsed immediately in running tap water. Samples were counterstained in hematoxylin for 1 min followed by a wash step in running tap water for about 3 min. Finally, sections were covered with a cover slip using Aquatex (Merk, Damstadt, Germany) and examined under the light microscope.

2.11. Periodic acid-Schiff staining

Glycogen content of PCLS was determined by the periodic acid-Schiff (PAS) staining as described previously by *Schaart* et al. with some modifications (Schaart et al., 2004). In brief, paraffin sections were deparaffinized and pretreated for 20 min in 1% periodic acid solution (Sigma, St. Luis, USA). Thereafter, sections were washed in mQ-water 3 times and incubated for 20 min in Schiff's reagent (Sigma, St. Luis, USA). Afterwards, sections were rinsed in tap water for 10 min. Finally, sections were counterstained with hematoxylin for 5 min and rinsed in tap water for 10 min. The sections were dehydrated and covered with a cover slip using Depex.

2.12. Hypoxia staining

Hypoxia staining was performed using the Hypoxyprobe-1 Plus Kit (Hypoxyprobe, Burlington, USA) according to the manufacturer's instructions. In brief, PCLS were incubated with 200 μM hypoxyprobe (2-pimonidazole HCl in 0,9% saline water) for 1 h prior to harvesting. Thereafter, PCLS were fixed in 4% formaldehyde/PBS and imbedded in paraffin. Paraffin sections of 4 μm thickness were deparaffinized and antigens were retrieved by incubation in citrate buffer (10 mM, pH = 6) for 20 min at 90 °C. After that, sections were incubated with the first antibody for 60 min at room temperature. Endogenous peroxidase activity was inhibited by incubation of the sections with 0.3% H_2O_2 in methanol for 20 min. Afterwards, the secondary antibody was applied for 30 min. Normal rat serum (NRS) (5%) was added to the secondary antibody to block non-specific binding. Antigen–antibody complexes were visualized by staining with di-aminobenzidine (DAB) chromogen with H_2O_2 for 20 min. Sections were counterstained with hematoxylin for 1 min. Following dehydration, the slides were covered with a cover slip using Depex and were examined under the microscope.

2.13. Statistics

A minimum of three different rat livers were used for each experiment, using slices in triplicates from each liver. Morphological scoring of every sample was performed by three independent researchers using the scale of staining intensity: 0—none, 1—weak, 2—moderate, 3-strong, and 4—very strong. For each separate staining method, the highest score was assigned to the section with the strongest staining, and therefore scores cannot be used to compare intensities of the staining of the different antigens. All samples were randomized and the scoring process was blind.

Table 1
The antibodies for the different immunostainings.

First antibodies	Source/clone	Company	Dilution	Secondary antibodies	Tertiary antibodies	Type of sections
Albumin	Mouse/mAb	Santa Cruz	1:50	RAMPO[a]	GARPO[b]	pf[d]
CD163 (ED2)	Mouse/mAb	AbD SeroTec	1:100	RAMPO	GARPO	cryo[e]
Collagen-type I	Rabbit/pAb	Rockland	1:200	GARPO	RAGPO[c]	cryo
Collagen-type III	Goat/pAb	Southern Biotech	1:100	RAGPO	GARPO	cryo
Cyp3a1	Rabbit/pAb	Chemicon	1:400	GARPO	RAGPO	pf
Cytokeratin-7	Mouse/mAb	Santa Cruz	1:50	RAMPO	GARPO	cryo
Desmin	Mouse/mAb	Sigma-Aldrich/	1:400	RAMPO	GARPO	pf
α-SMA	Mouse/mAb	Sigma-Aldrich	1:1000	RAMPO	GARPO	pf
Vimentin	Mouse/mAb	Dako	1:50	RAMPO	GARPO	pf
Ki-67	Rabbit/pAb	Monosan	1:500	GARPO	RAGPO	cryo

[a] RAMPO (rabbit anti-mouse peroxidase conjugated antibody, DAKO, Denmark)
[b] GARPO (goat anti-rabbit peroxidase conjugated antibody, DAKO Denmark)
[c] RAGPO (rabbit anti-goat peroxidase conjugated antibody, DAKO, Denmark)
[d] paraffin sections
[e] cryosections

Continuous variables are expressed as means ± SEM. Morphological scores are expressed as median and interquartile range. Statistical testing was performed with two way repeated measures ANOVA with individual rats as random effect. We performed a Tukey HSD post-hoc test for pairwise comparisons. A p-value of ≤0.05 was considered to be significant. In all graphs the mean values and standard error of the mean (SEM) are shown.

3. Results

3.1. Viability of slices during prolonged incubation

The viability of the PCLS following 120 h incubation was assessed by LDH leakage and ATP content (Fig. 1a,b). According to the obtained results, slices retained the ability to synthesize ATP at least up to 120 h incubation: the mean value of ATP content in slices incubated in WME and RegeneMed® after 120 h incubation was 13.07 and 9.14 pmol/μg protein respectively, whereas fresh slices contained 11.19 pmol/μg protein. Slices incubated in RegeneMed® had a consistently lower ATP level over time compared to WME ($p = 0.048$). However, the incubation time had no effect on ATP levels ($p > 0.05$).

We observed an initial decrease in LDH leakage of 9–11% after 24 h. Thereafter the LDH leakage remained relatively stable at 4–6% per day. The elevated LDH leakage during the first hours of incubation can be explained by the damage of the outer cell layers during the slicing and handling procedures. No difference observed in LDH leakage between slices incubated in WME and RegeneMed® ($p > 0.05$). Remarkably, the protein content of PCLS decreased gradually over five days of incubation in both media ($p < 0.001$). Protein content was preserved better in RegeneMed® than in WME ($p < 0.001$).

3.2. Morphological changes in PCLS during 120 h incubation

The viability of PCLS following incubation up to 120 h was also assessed by histomorphology (Fig. 2). The morphological evaluation of fresh slices showed that the normal liver architecture was well preserved after the slicing procedure. Upon prolonged incubation in both media, the slices showed a higher cell density. Hepatocytes were smaller, rounded-off and their cytoplasm appeared more homogenous. Sinusoids were substantially narrowed after 120 h of incubation. After 24 h of incubation the slices were surrounded with a thin layer of dead cells, however, no extensive necrosis was observed inside the slices. At 120 h, slices incubated in WME contained viable hepatocytes without distinct lobular architecture. Occasional non-specifically localized small necrotic areas were observed. With time, the PCLS gradually decrease in diameter and increase in thickness ($p < 0.001$), which was much more pronounced in slices incubated in RegeneMed® medium (up to 3 fold increase in thickness), than in WME (up to 1.5 fold) (Figs. 1d, 2a,b,c) (p for difference < 0.001; p for interaction medium and time < 0.001). The increase in thickness in RegeneMed® was accompanied by the formation of big necrotic regions in the inner part of the tissue. Moreover, hypoxia staining revealed the development of hypoxic regions inside the slices incubated in RegeneMed® following 72 h incubation and longer, that suggests insufficient oxygen delivery to the inner part of the thickened slices (Fig. 2f). Nevertheless, a part of the tissue surrounding the necrotic region contained viable hepatocytes. A few mitotic figures were observed in the slices, revealing regeneration. This process was more pronounced in slices incubated in RegeneMed® medium than in WME.

3.3. Cell proliferation

Ki-67 staining revealed an increase in proliferation rate of different cell types, both parenchymal and NPCs in both media, which was

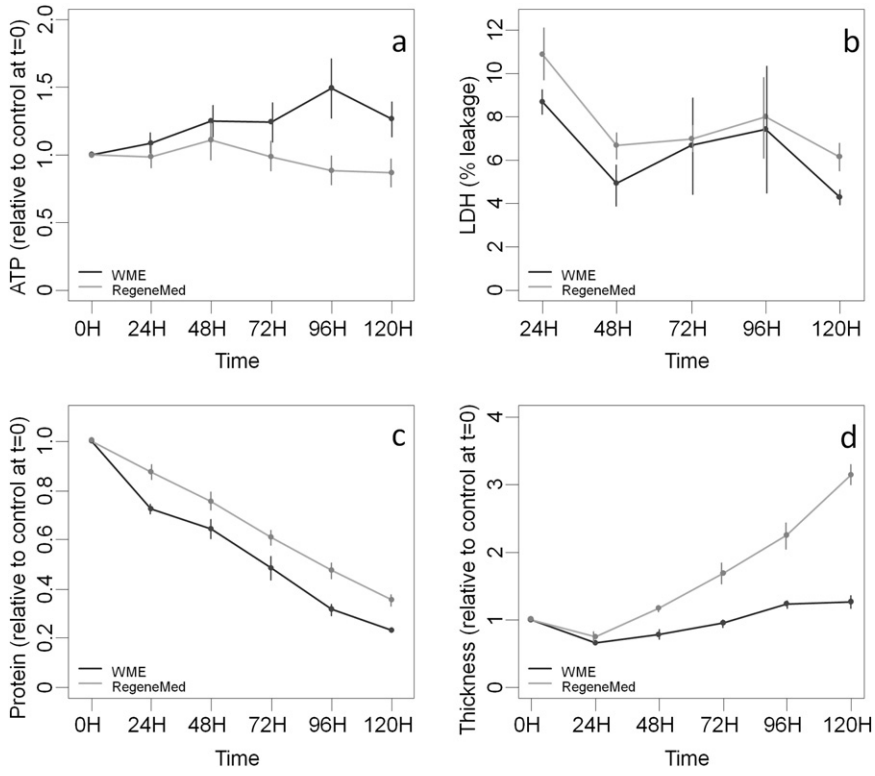

Fig. 1. Viability during 120 h incubation indicated by the ATP content (a), LDH leakage (b), protein content per slice (c) and thickness (d) of slice in two different media (WME (black) and RegeneMed® (gray)). The ATP (pmol/μg protein), the protein content (mg protein/slice) and the thickness are expressed as relative values to the control slices at the beginning of incubation. The LDH leakage is expressed as a percentage of the total LDH content in the slice. Data represent the average ± SEM of 4–9 experiments (ATP), 3 experiments (LDH leakage and thickness) and 4–12 experiments (protein content), using 3 PCLS for each group in every experiment.

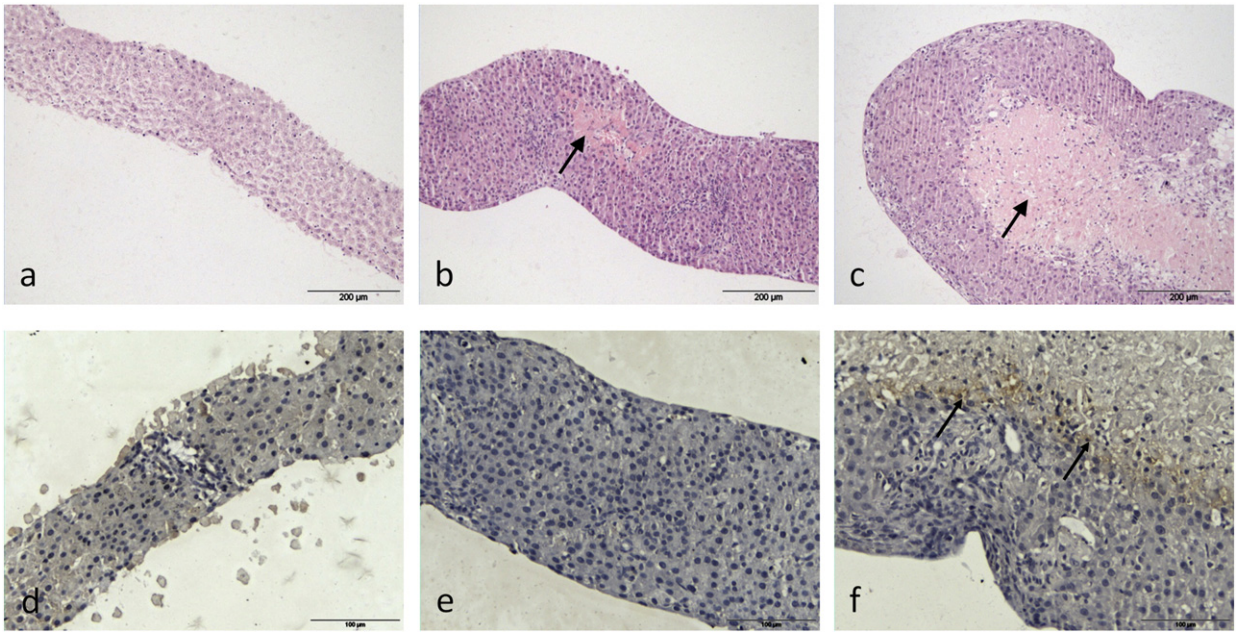

Fig. 2. Cross-sections of PCLS at 0 h (a) and incubated 120 h in WME (b) or RegeneMed® (c). Sections were stained with hematoxylin–eosin. Arrows indicate necrotic zones/areas. Hypoxia staining performed on PCLS incubated for 24 (d) and 120 h (e) in WME or 120 h in RegeneMed® (f). Representative images are shown. Arrows indicate hypoxic zones. For a, b, c bar = 200 μm. For d, e, f bar = 100 μm.

further confirmed by immunostaining for specific cell types, such as fibroblasts, HSCs, KCs and BECs (Fig. 3).

3.4. The outer cell lining

Remarkably, the formation of a cell lining/border around the slices incubated for 72 h in RegeneMed® was observed. The lining consisted of slightly flattened cells. Such lining was also observed around slices incubated in WME, although less prominent and only after 96 h of incubation.

The newly formed cell lining closely resembled the Glisson's capsule of the liver, which consists of a single layer of mesothelial cells. To identify the nature of the newly formed outer cell lining, sections from the slices incubated for 120 h in the two media were immunostained with antibodies raised against desmin and vimentin, which are classical mesenchymal cell markers (Cassiman, 2002), and antibodies against MHC class II molecules, which are known to be well expressed by mesothelial cells and some epithelial cells (Mutsaers, 2002; Rose, 2001; Valle, 1995).

Indeed, some flattened cells of the outer layer stained positively for vimentin and MHC class II. Furthermore, single MHC class II—positive cells and numerous vimentin—positive cells were observed close to

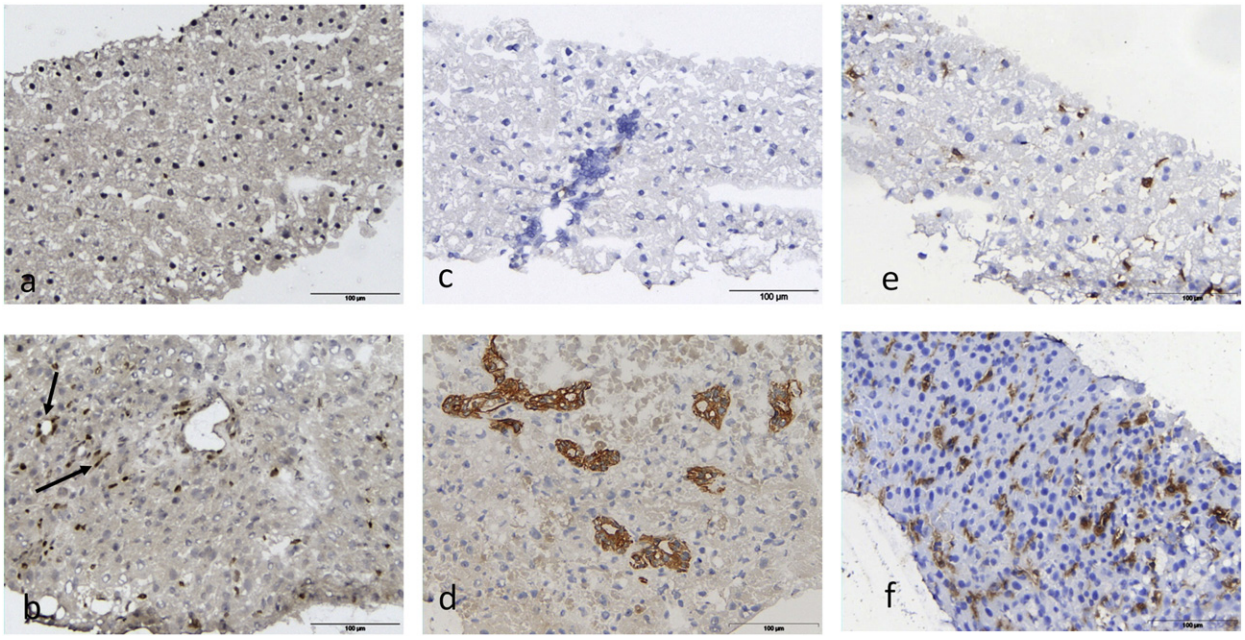

Fig. 3. Ki-67 staining on cross-sections of PCLS at 0 h (a) and incubated 120 h in WME (b). Arrows indicate dividing cells. The same was seen in slices incubated in RegeneMed® (results not shown). Staining of the bile ducts (CK-7) on slices at 0 h (c) and incubated 96 h in Regenemed® (d). Pictures are similar for slices incubated in WME (not shown). ED2 (Kupffer cells) staining on PCLS at 0 h (e) and incubated in WME for 120 h (f). Pictures are similar for RegeneMed® (not shown). Bar = 100 μm.

the outer cell lining. Only a few cells of the outer cell lining stained positively for desmin at 120 h of incubation. Remarkably, more cells of the newly formed lining were desmin-positive at 72 h of incubation in some of the sections (Fig. 4).

In order to compare the immunohistochemical expression profiles of the newly formed cell lining with the mesothelial cells of the Glisson's capsule, we performed the same set of immunostainings on sections containing normal rat liver capsule. The results indicate that the mesothelial lining of the capsule showed the same staining for vimentin, desmin and MHC class II as the newly formed lining (data for the liver capsule is not shown).

3.5. Development of fibrosis

The development and severity of fibrosis in PCLS following five days of incubation in the two media were assessed in this study. Accordingly, collagen I and collagen III deposition, as well as proliferation and activation of hepatic stellate cells and fibroblasts were evaluated by immunostaining. Collagen I and III are generally considered as major ECM proteins in the fibrogenic process. Moreover, it was shown that their deposition in the liver tissue changes notably from the early to the late stage of fibrosis (Chen et al., 2014).

The immunostaining for α-SMA revealed an increase in the number of myofibroblasts following 120 h of incubation in comparison with non-incubated slices. In 0 h slices, desmin and α-SMA-positive cells were noted only around the hepatic artery and portal vein. With the development of fibrosis, we observed a considerable increase in the intensity of α-SMA and desmin staining in the portal area with proliferating bile ducts. The appearance of α-SMA and desmin positive cells was also seen at later time points in the parenchyma between hepatocytes and in the necrotic areas (Fig. 5).

Furthermore, it was shown that collagen I and collagen III deposition increased significantly following 120 h of incubation irrespectively of the medium type ($p = 0.02$ and $p < 0.001$ respectively, Fig. 5, Fig. 6). In non-incubated slices collagen I and III deposition was observed predominantly around the portal vein, bile ducts and hepatic vein, and only a few very thin collagen fibers were observed in some areas of the parenchyma. After the prolonged incubation, collagen accumulation in the parenchyma became more intensive: dark thick fibers were well visible between hepatocytes (Fig. 5). Collagen deposition was prevalent in portal and periportal areas, which was accompanied by a 20-fold increase in bile duct proliferation after 120 h of incubation compared to the 0 h control ($P < 0.001$, Fig. 3c and d, Fig. 6).

In this study, the proliferation and activation of Kupffer cells were assessed by ED2 immunostaining. Accordingly, the staining intensity increased significantly when comparing 120 h of incubation to 0 h control in both media ($p < 0.001$, Fig. 3e and f, Fig. 6).

3.6. Lipid homeostasis

Along with fibrosis development, also lipid accumulation took place in liver slices during prolonged incubation. Fat droplets of various sizes were detected in slices incubated in WME without particular zonal localization. In slices incubated in RegeneMed®, fat was primarily deposited in the inner necrotic part, whereas hepatocytes in the outer cell layers showed low fat content. Incubation over time resulted in a significant increase in fat content ($p = 0.002$), and was more pronounced in slices incubated in RegeneMed® medium than in WME ($p = 0.0469$, Figs. 6, 7).

3.7. Functional characterization of PCLS

Albumin expression by hepatocytes is a commonly used parameter to characterize their function. Hepatocytes in freshly fixed slices highly expressed albumin (Fig. 8a). Staining was rather homogenously distributed over the slice. Some parts of the slices revealed patchy distribution of albumin. After 5 days of incubation in WME immunohistochemistry staining revealed patchy albumin distribution: some cells were negative, while others showed high albumin expression. Slices incubated in RegeneMed® contained fewer positive cells after 5 days of incubation than slices incubated in WME. Most of the intact hepatocytes in the outer cell layers were negative (Fig. 8b and c).

In normal conditions with constant oxygen and nutrient supply, glycogen is stored in hepatocytes and serves as a secondary energy source. Slices fixed at 0 h showed high homogeneous glycogen deposition (Fig. 8d). Following incubation, glycogen levels decreased significantly

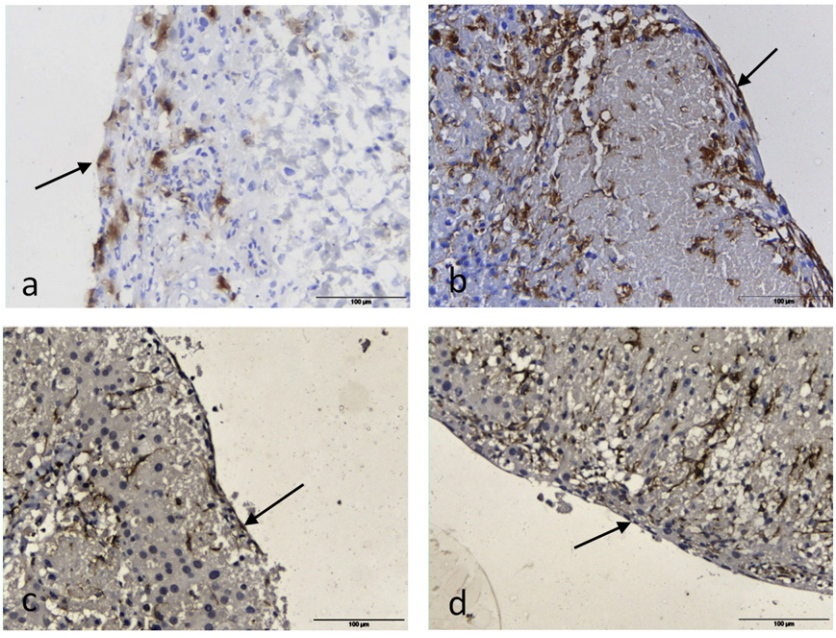

Fig. 4. Staining for MHC class II (a), vimentin (b) of the outer cell lining in PCLS incubated for 120 h in RegeneMed® and for desmin on PCLS incubated for 72 h (c) or 120 h (d) in RegeneMed®. The same was seen in slices incubated in WME. Bar = 100 μm.

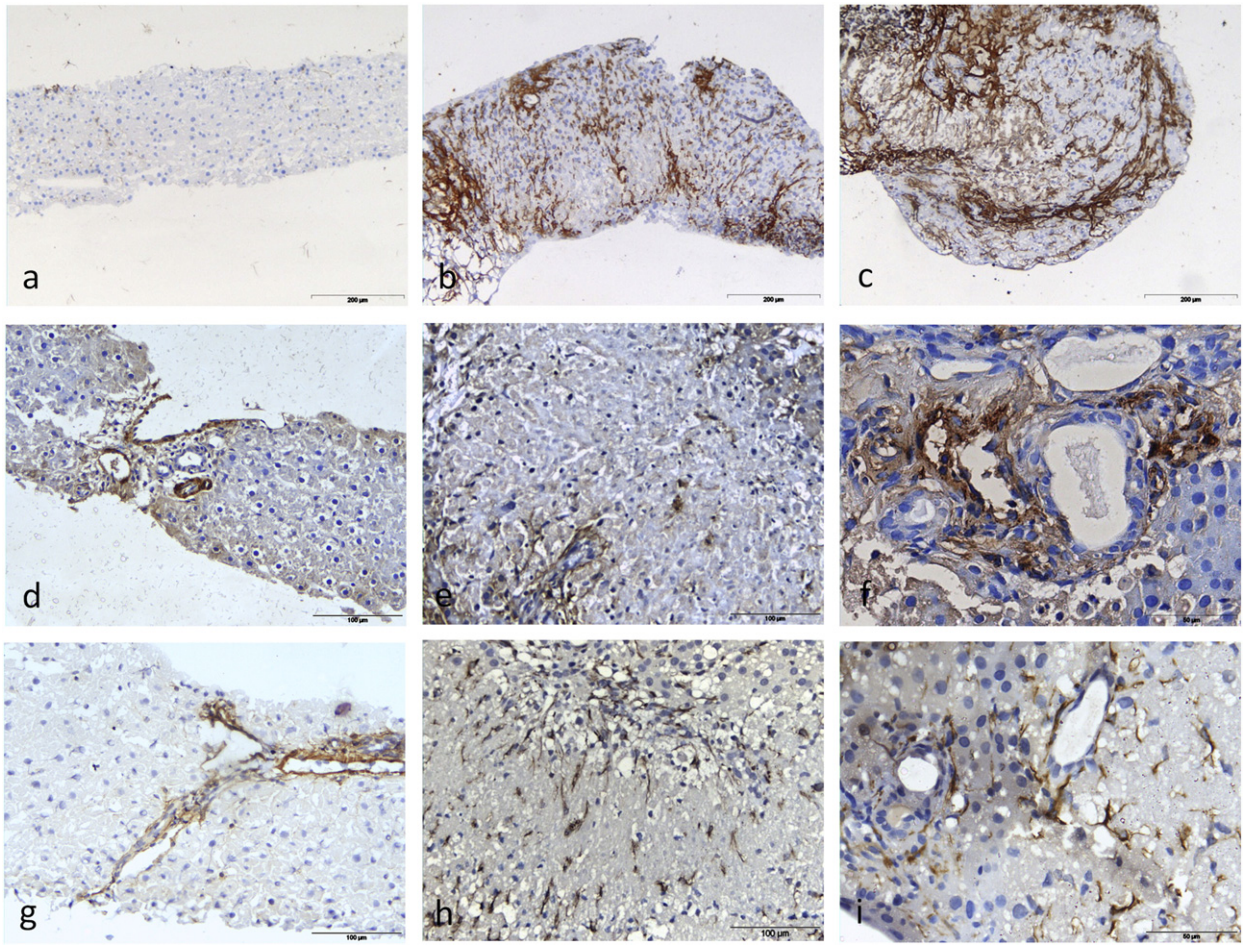

Fig. 5. Collagen III staining on cross-sections of PCLS at 0 h (a) and incubated 120 h in WME (b) or RegeneMed® (c). Pictures are similar for Collagen I (not shown). Immunostaining for α-SMA on PCLS at 0 h (d) and incubated in RegeneMed® (e) or WME (f) for 120 h. Desmin staining performed on PCLS at 0 h (g) and incubated for 120 h in RegeneMed® (h, i). Pictures show the portal area (d, g), the area with extensive bile duct proliferation (f, i) and a necrotic zone (e, h). For a, b, c: bar = 200 μm. For d, e, g, h: bar = 100 μm. For f, i: bar = 50 μm.

in slices incubated in WME (<10% of cells were positive at 120 h), showing patchy localization of the glycogen. In slices incubated in RegeneMed® medium glycogen levels were shown to be preserved longer and better, mostly in the outer layers of hepatocytes, whereas the inner necrotic part of the slices did not show any PAS-positive staining (Fig. 8e and f).

Finally, it was demonstrated that the expression levels of Cyp3a1, the main Cyp3a form in rat liver (Martignoni, 2006), were still preserved after 5 days of incubation. Cyp3a1 expression dropped following 24 h by approximately 50–60% in both media, but these levels were well preserved during 5 days of incubation (Figs. 6, 8). A decrease in expression levels was found to be significant over time ($p < 0.001$) with no medium effect (Fig. 6).

4. Discussion

The PCLS model is widely used nowadays to study xenobiotic metabolism and toxicity (de Graaf et al., 2007; Groothuis et al., 2014; Vickers and Fisher, 2013). However, most studies have been performed for 24–48 h and no extensive studies have been done to characterize morphological changes observed in the liver slices during prolonged culture time. In this study, we examined the morphological changes in PCLS, including both parenchymal and non-parenchymal cell markers, during 5 days of incubation and compared the effect of two different media on slice viability and morphology ex vivo.

4.1. Viability of the various cell types in the slices during prolonged incubation in two different media

The viability of all cell types in the slices was preserved during 5 days of incubation in both media, which was reflected by morphology, ATP content and LDH leakage. However, slices incubated in WME preserved higher ATP levels compared to those in RegeneMed® medium. These lower ATP levels in slices incubated in RegeneMed® medium may be explained by the formation of the large necrotic regions in the inner part of the slices. KCs, BECs, HSCs and fibroblasts remained present during incubation of the slices and were able to proliferate, indicating their viability.

4.2. Morphological changes in the PCLS following prolonged incubation in two different media

During prolonged incubation, slices underwent notable tissue remodeling. For example, PCLS increased in thickness and decreased in diameter, which was accompanied by a profound loss of proteins. Slices incubated in RegeneMed® were affected more in comparison with WME: the increase in thickness was shown to be 2.5 times higher in RegeneMed® than in WME. The protein content of the slices decreased gradually during incubation. Previous studies reported the drop in protein content of rat slices up to 53–76% of 0 h levels following 3 days of incubation (Price et al., 1998; Toutain et al., 1998). In our study, the protein content of the slices was preserved by 50 and 62% at 72 h and by 23

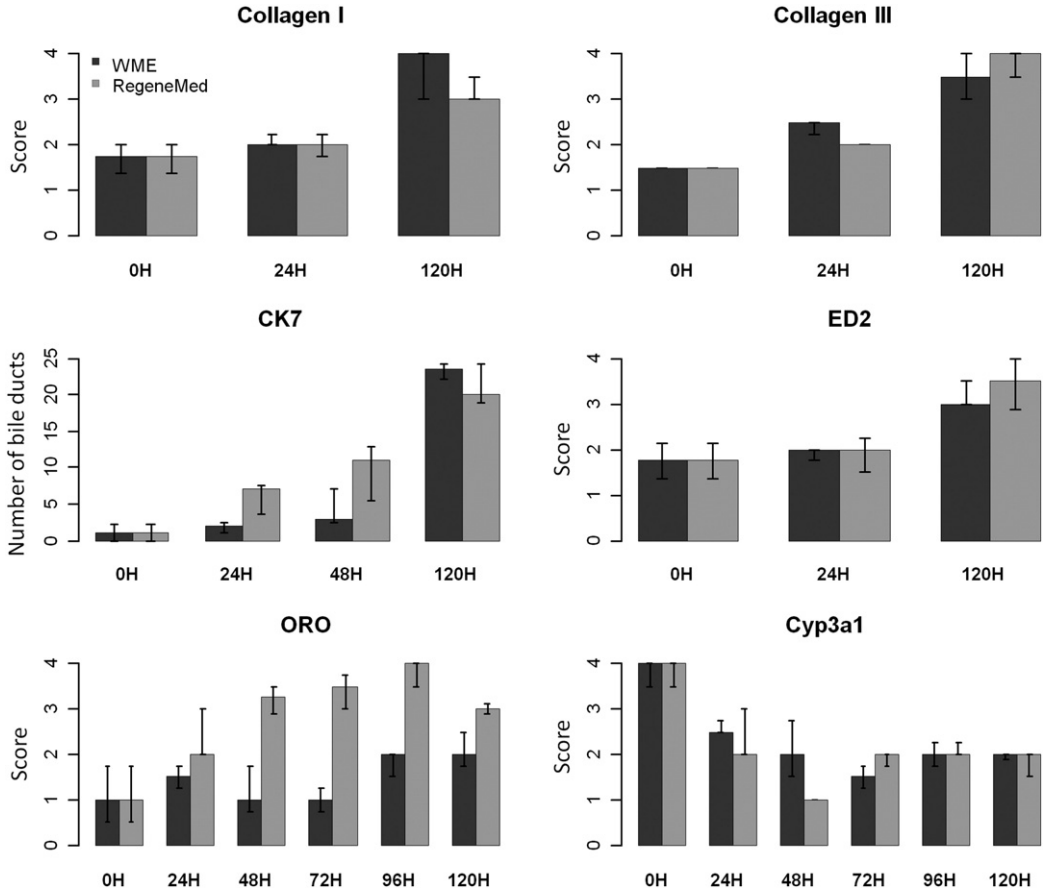

Fig. 6. Quantification of the staining of Collagen I, III and fat deposition in PCLS following 120 h incubation in WME or RegeneMed® and of ED2 and Cyp3a1 expression in PCLS over 120 h incubation in WME or RegeneMed®; The number of bile ducts in slices incubated for 0, 24, 48 or 120 h in WME or RegeneMed®. Collagen I and III, ED2, ORO and Cyp3a1 data expressed as a score (0–4). The scoring is based on quantitative comparisons of staining intensities using a randomized blinded method. All numbers are expressed as median (with interquartile range) of 3–4 experiments, using 3 PCLS for each group in every experiment.

and 35% at 120 h for WME and RegeneMed® respectively. This decrease in the slice protein content can be explained by the detachment of outer cells at the beginning of incubation prior to the capsule formation, as well as by induction of autophagy later on. Autophagy has been shown to contribute significantly to the development of fibrosis, playing both a profibrogenic role (activation of HSCs) and a protective role (activation of cyto-protective mechanisms in hepatocytes and anti-inflammatory processes in KCs) (Bhogal and Afford, 2013; Cursio, 2015; Mallat, 2014; Song, 2014). Moreover, the observed increase in the number of hepatocytes per area during incubation suggests the ongoing autophagic processes in the tissue (Fig. 2a,b,c).

Hampered oxygen and nutrient diffusion through the increased number of cell layers in slices incubated in RegeneMed® is the likely cause of the formation of hypoxic and necrotic zones inside the slices. In slices incubated in WME where the increase in thickness was about 1.5 fold, only occasional necrotic areas were seen without any zone specificity. The reason and exact mechanism of these changes in configuration are not clear. Gradual increase in slice thickness and gradual decrease in diameter in time rule out that folding of the slices is responsible for this. Ki-67 revealed an increase in proliferation of the different cell types. However, it is unlikely that this proliferation is solely responsible for such a rapid slice thickening. Therefore, we speculate that the cells are moving inside the slice during incubation, leading to the observed configurational changes. Collective cell migration has been shown to play a role in embryonic development and tissue regeneration (Friedl, 2009; Ilina, 2009; Lange and Fabry, 2013; Vasilyev et al., 2009). During the reported collective cell migration, cells move as a group, preserving their cell–cell junctions and polarity. For example, this process has been observed in zebrafish embryogenesis (primodium migration and nephron formation), carcinogenesis (cell migration in colorectal

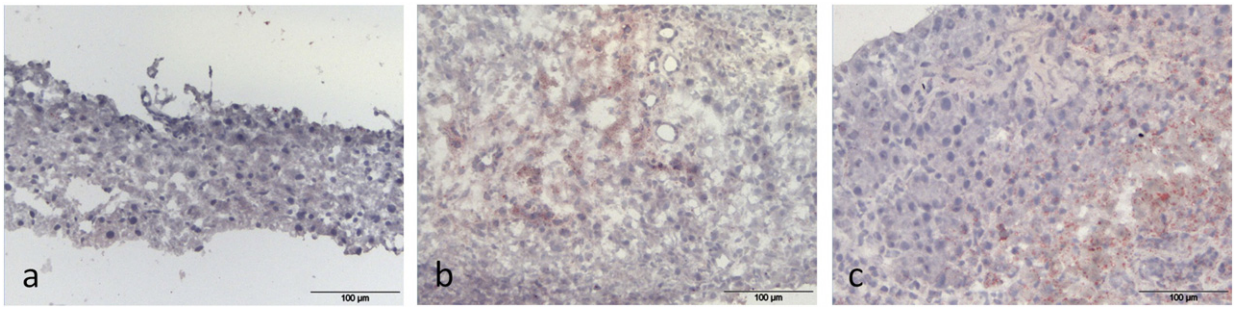

Fig. 7. ORO (fat) staining on cross-sections of PCLS at 0 h (a) and incubated 120 h in WME (b) or RegeneMed® (c). Bar = 100 µm.

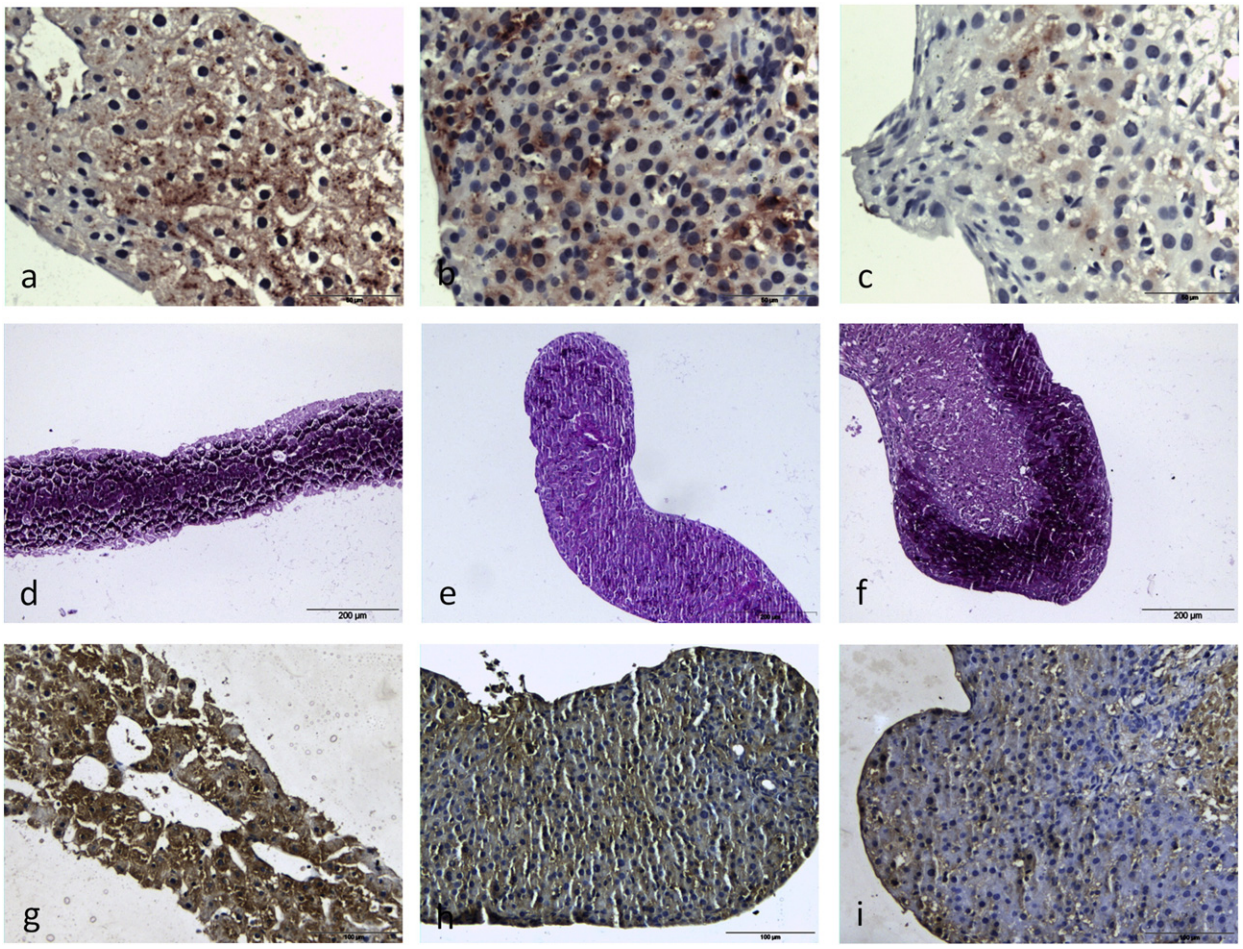

Fig. 8. Albumin staining on cross-sections of PCLS at 0 h (a) and incubated 120 h in WME (b) or RegeneMed® (c). PAS (glycogen) staining on cross-sections of PCLS at 0 h (d) and incubated 120 h in WME (e) or RegeneMed® (f). Cyp3a1 staining on cross-sections of PCLS at 0 h (g) and incubated 120 h in WME (h) or RegeneMed® (i).For a, b, c bar = 50 µm; for d, e, f bar = 200 µm, for g, h, I bar = 100 µm.

carcinoma, breast cancer, fibrosarcoma etc.), as well as wound healing (skin and corneal epithelium regeneration). Configurational changes observed in the slices might be an adaptation response to the physical stress provided during continuous shaking of the incubation plates, or to release of EGF or TNFα, as liver epithelial cell migration was shown to be influenced by these growth factors, which are critical regulators in hepatocyte proliferation and liver regeneration (Bade and Feindler, 1988; Geimer, 1991; Natarajan et al., 2007).

In addition to the changes in size and shape, the formation of a new cell lining was observed around the slices following 72–96 h of incubation. Therefore, we wanted to investigate the nature of this newly formed cell lining around the slices after the prolonged incubation, which to our knowledge has not been described before. Morphological examination of the outer cell lining and the mesothelial lining of the Glisson's capsule revealed a close resemblance. Both linings are formed with a monolayer of elongated flattened cells with a central round or oval nucleus, which rest on the basement membrane. Mesothelial cells are cells with an intermediate character between epithelial and mesenchymal cells, exhibiting properties and expressing markers of both cell types (Chau, 2012; Li, 2013). In our study, it was shown that the mesothelial layer of the Glisson's capsule was positive for vimentin and MHC class II, and occasionally positive for desmin, which is in accordance with the literature data (Ijzer, 2006; Valle, 1995). The cell monolayer around the PCLS after prolonged incubation showed a similar immunohistochemical expression profile as the mesothelial lining of Glisson's capsule. Therefore we speculated that this cell lining is of mesothelial nature, since it shows both epithelial characteristics (formation of a monolayer structure) and mesenchymal characteristics (positive staining for vimentin), as well as positive staining for MHC class II molecules, which are usually well expressed on mesothelial cells.

In order to understand the origin of the formed cell lining, we hypothesize that the cell lining is related to mesothelium. The origin of regenerative mesothelial cells is still unknown, but several hypotheses have been proposed, including transformation of serosal macrophages, centripetal migration of mesothelial cells, exfoliation of cells from adjacent sites and transformation from mesenchymal precursors (Mutsaers, 2002). Since there is no parietal environment in our system and no mesothelium is presents in the PCLS, the first three hypothesis can be ruled out. On the other hand, transformation of the mesenchymal cells inside the slice into the mesothelial cells seems to be possible. This mesenchymal–epithelial transition (MET) hypothesis was described already earlier (Lewis, 1923) and found support in the recent in vivo study in rats (Nishioka, 2008). In the latter study, a new layer of flattened vimentin-positive spindle-shaped cells, which morphologically resemble mesothelial cells, was formed on the liver surface 5 days after the removal of peritoneum. The role of MET in tissue regeneration received much attention recently (Michelotti et al., 2013; Yang, 2008). However, even though there are findings supporting this transition, this subject remains highly controversial (Chau, 2012; Xie, 2013).

The question may arise whether the cell lining might be formed by fibroblasts, since it was shown before that MHC class II expression can be induced in fibroblasts (Boots, 1994; Rose, 2001). However, fibroblasts do not form monolayers and are not restricted by a polarizing attachment to a basal lamina on one side (Acton, 2013), as was observed

in this study in PCLS. Moreover, a decrease in the number of the desmin-positive cells on the surface of the slices from 3 to 5 days of incubation, suggests the gradual loss of the mesenchymal characteristics by the outer cells.

The migration of ED-2 positive cells towards the slice surface was observed in this study. The same phenomenon was described previously during the process of mesothelial healing (Nishioka, 2008). It was suggested that the recruited macrophages are ultimately replaced by the mesothelial-like cells and they play a key role in the stimulation of fibroblasts migration to the wound (DiZerega et al., 1997).

The formation of a capsule-like cell lining around the PCLS during prolonged incubation in both media might function as a protective barrier to the slices, shielding them from the environment and/or microorganism invasion. Moreover, the newly formed cell capsule might influence the transport of fluids and nutrients, as well as initiation of inflammation responses.

Changes in lobular liver structure were accompanied with an increase in proliferation of mesenchymal cells and bile ducts. In addition, the development of fibrosis was observed in PCLS with the gradual increase in collagen deposition over 5 days, in line with previous observations by us (van de Bovenkamp et al., 2008; Westra et al., 2014) and others (Vickers et al., 2004). In vivo, the pattern of fibrosis depends on the etiology of the injury. Hepatotoxins usually trigger the development of centrolobular fibrosis, associated with activation of HSCs, whereas in case of bile duct obstruction, the development of portal fibrosis with the extensive bile duct proliferation can be observed which primary involves activation and proliferation of portal fibroblasts (PFs) (Bataller and Brenner, 2005; Guyot, 2007a; Guyot, 2007b). In the PCLS model, we observed changes distinctive for the bile duct ligation model, such as bile duct proliferation and extensive extracellular matrix deposition in the portal areas (Clouzeau-Girard, 2006). Formation of new bile ducts was observed not only in the portal areas, but in other areas as well. The increase in the number of bile ducts can be viewed as a compensatory mechanism to facilitate the elimination of bile, which might be hindered by the formation of a new cell lining around the slice.

A significant increase in the number of α-SMA-positive cells in the areas of bile duct proliferation indicates the differentiation of PFs towards myofibroblasts (MFs). These observations are in line with the described earlier "ductular reaction", where bile duct proliferation act as a "pacemaker" in the development of fibrosis (Burt, 1993; Yoshioka, 2005). It is known that BECs produce cytokines, which stimulate fibroblasts proliferation and differentiation towards MFs leading to the deposition of extracellular matrix in portal areas (Guyot, 2007b). Besides proliferation and differentiation of PFs towards MFs, an activation of HSCs was observed, that was supported by an increase in the intensity of vimentin, desmin and α-SMA staining (Kara et al., 2009). Also the collagen I and collagen III data are in line with the findings of the desmin and α-SMA staining, as collagen deposition prevailed in the areas of bile duct proliferation. However, at the late stage of incubation, collagen deposition increased dramatically in the parenchyma as well. The differences in PCLS remodeling observed in two different media were well reflected in the prevalence of collagen deposition in different slice areas. Accordingly, deposition of collagen in slices incubated in WME medium was predominant in areas with bile duct proliferation. Whereas, in PCLS incubated in RegeneMed® medium excessive collagen deposition was concentrated in the outer cell ring containing intact hepatocytes. It is important to stress that collagen deposition is known to be involved not only in fibrotic liver diseases, but also in adaptive and beneficial processes, such as liver regeneration (Yamamoto et al., 1995).

As a result of the thickening of the slices incubated in RegeneMed® medium, the inner areas of the slices became hypoxic, probably due to the limited oxygen diffusion. The band of hypoxic cells in the inner part of the slices was observed already after 72 h of incubation. Slices incubated in WME did not increase in thickness to the extent that could prevent oxygen to reach the inner cell layers. A small hypoxic area was observed in one liver slice only at 120 h of incubation in WME. Hypoxia can play a role in fibrosis development and progression, as hypoxic stress stimulates the over-expression of HIF-1α, which can lead to HSC/MF migration and activation by regulating different signaling pathways (Zhan, 2015). In line with this hypothesis, the increased number of α-SMA and desmin-positive cells were localized in the hypoxic/necrotic regions in the inner part of the slices incubated in RegeneMed®.

Another process observed in the PCLS during prolonged incubation is accumulation of fat in the hepatocytes. Under normal conditions, mitochondrial β-oxidation is the primary way for the removal of fatty acids (FA). The disturbance of this process due to, for example, oxidative stress can lead to the development of liver steatosis (Nassir, 2014; Oliveira, 2006; Vickers, 2006; Wei, 2008). High oxygen tension, which is crucial for the slice viability, can result in slight oxidative stress and an increase in ROS production (Martin, 2002). This can ultimately trigger the pathological cascade of fat accumulation. Furthermore, the activation of Kupffer cells that was observed in our study, may have contributed to the fat accumulation by inducing the TNF-α and IL-β pathways (Suzuki, 2014; Wei, 2008).

The high content of glucose in culture media (25 mM in WME) could have contributed to fat accumulation in the slices. During excessive energy supply, increased hepatic malonyl-CoA levels suppress FA oxidation and at the same time stimulate their *de novo* synthesis (Wei, 2008). In addition, high glucose levels can stimulate the HSC proliferation and collagen I production via MAP kinase pathway activation by ROS (Sugimoto, 2005). A significant accumulation of fat observed in the hypoxic/necrotic regions of the slices incubated in RegeneMed® can be explained by the influence of HIFs on lipid metabolism and fatty liver formation, which was shown previously (Suzuki, 2014). It was reported that HIF-2 increases cellular lipid deposition. This process primary involves an impairment of FA β–oxidation and an increase in lipid storage capacity.

4.3. Functional characterization of PCLS incubated in two different media

The decrease in the activity of drug metabolizing enzymes is one of the main limitations in the use of hepatocyte cultures for metabolism and toxicity studies. Depending on the culture conditions, the Cyp activity in cultured hepatocytes dramatically decreases to very low levels in 24–48 h cultures whereas the activity is somewhat better preserved in sandwich cultures. A decrease in Cyp metabolism in PCLS *ex vivo* was already described before (Price et al., 1998; Toutain et al., 1998) but the decrease is not as rapid as in cultured hepatocytes. After an initial drop of Cyp3a1 expression by hepatocytes during first 24 h of incubation, the expression remains stable for up to five days in both media. These findings give support to PCLS as a model for prolonged drug metabolism and toxicity studies. Further studies are currently in progress to measure the functionality of the expressed metabolic enzymes.

Glycogen content in slices incubated in WME decreased substantially over time, which can be explained by the absence of insulin in the medium, which facilitates the uptake of glucose to the slices. In RegeneMed® medium, which contains insulin, glycogen was preserved better, particularly in the outer layers of healthy hepatocytes. However, the decrease in glycogen content in rat liver slices during incubation was described before, even in the presence of insulin (Toutain et al., 1998).

Albumin content of the slices dropped significantly over five days of incubation in both media. However, a larger amount of hepatocytes expressing albumin were detected in slices incubated in WME compared to RegeneMed®. Future studies will elucidate to what extent the slices still produce and excrete albumin after 5 days of incubation.

5. Conclusions

In conclusion, we showed that all cell types in the slices remained present and viable over 5 days of incubation, despite formation of

necrotic areas when slice thickness increased too much. However, during this period, slices undergo substantial tissue remodeling, accompanied by the development of fibrosis, bile duct proliferation and fat deposition. Due to the extensive collagen deposition, we suggest that prolonged incubation of PCLS can be used as a fibrosis model to study fibrosis development and test possible antifibrotic treatments.

Importantly, the presence and viability of NPCs were maintained over five days of incubation, which supports the use of PCLS for five-day toxicity studies. Interestingly, cell migration can take place *ex vivo* and formation of a new capsule-like cell lining was observed following prolonged PCLS incubation, which to our knowledge have not been reported before. The precise molecular mechanism that triggers and propagates formation of this cell lining requires further investigation, but MET may be involved.

Finally, the observed changes in slice viability, morphology and function were quantitatively different in the two media, WME and RegeneMed®, indicating that a more rich medium does not necessarily result in improved viability and function of rat PCLS. Our results emphasize the importance of media selection for any given study with tissue slices. Moreover, changes occurring in PCLS *ex vivo* have to be taken into account when interpreting the obtained results from toxicological or pharmacological studies.

Conflict of interest

The authors have no conflicts of interest to report.

Transparency document

The Transparency document associated with this article can be found, in online version.

Acknowledgements

This study was financially supported by the EU-funded project NanoBio4Trans (Grant no. 304842).

References

Acton, A.Q., 2013. Heart Failure: New Insights for the Healthcare Professional. 2013th ed. (Atlanta, Georgia, USA).
Bade, E.G., Feindler, S., 1988. Liver epithelial cell migration induced by epidermal growth factor or transforming growth factor alpha is associated with changes in the gene expression of secreted proteins. In vitro cell. Dev. Biol. 24 (2), 149–154.
Bataller, R., Brenner, D.A., 2005. Liver fibrosis. J. Clin. Invest. 115 (2), 209–218.
Bhogal, R.H., Afford, S.C., 2013. Autophagy and the liver. In: Bailly, Y. (Ed.), Autophagy—A Double-Edged Sword—Cell Survival or Death?InTech, Croatia.
Boots, A.M., 1994. Antigen-presenting capacity of rheumatoid synovial fibroblasts. Immunology 82 (2), 268–274.
Burt, A.D., 1993. Bile duct proliferation—its true significance? Histopathology 23 (6), 599–602.
Cassiman, D., 2002. Hepatic stellate cell/myofibroblast subpopulations in fibrotic human and rat livers. J. Hepatol. 36 (2), 200–209.
Catania, J.R., 2007. Induction of CYP2B and CYP2E1 in precision-cut rat liver slices cultured in defined medium. Toxicol. in Vitro 21 (1), 109–115.
Catania, J.M., Parrish, A.R., Kirkpatrick, D.S., Chitkara, M., Bowden, G.T., Henderson, C.J., et al., 2003. Precision-cut tissue slices from transgenic mice as an in vitro toxicology system. Toxicol. in Vitro 17 (2), 201–205.
Chan, C., 2002. Metabolic pre-conditioning of cultured cells in physiological levels of insulin: generating resistance to the lipid-accumulating effects of plasma in hepatocytes. Biotechnol. Bioeng. 78 (7), 753–760.
Chan, C., Berthiaume, F., Lee, K., Yarmush, M.L., 2003. Metabolic flux analysis of hepatocyte function in hormone- and amino acid-supplemented plasma. Metab. Eng. 5 (1), 1–15.
Chau, Y.Y., 2012. The role of Wt1 in regulating mesenchyme in cancer, development, and tissue homeostasis. Trends Genet. 28 (10), 515–524.
Chen, W., Rock, J.B., Yearsley, M.M., Ferrell, L.D., Frankel, W.L., 2014. Different collagen types show distinct rates of increase from early to late stages of hepatitis C-related liver fibrosis. Hum. Pathol. 45 (1), 160–165.
Clouzeau-Girard, H., 2006. Effects of bile acids on biliary epithelial cell proliferation and portal fibroblast activation using rat liver slices. Lab. Investig. 86 (3), 275–285.
Cursio, R., 2015. The role of autophagy in liver diseases: mechanisms and potential therapeutic targets. Biomed. Res. Int. 2015.
de Graaf, I.A.M., van der Voort, D., Brits, J.H.F.G., Koster, H.J., 2000. Increased post-thaw viability and phase I and II biotransformation activity in cryopreserved rat liver slices after improvement of a fast-freezing method. Drug Metab. Dispos. 28 (9), 1100–1106.
de Graaf, I.A.M., Groothuis, G.M.M., Olinga, P., 2007. Precision-cut tissue slices as a tool to predict metabolism of novel drugs. Expert Opin. Drug Metab. Toxicol. 3 (6), 879–898.
de Graaf, I., Olinga, A.M., de Jager, P., Merema, M.H., de Kanter, M.T., R. van de Kerkhof, E.G., et al., 2010. Preparation and incubation of precision-cut liver and intestinal slices for application in drug metabolism and toxicity studies. Nat. Protoc. 5 (9), 1540–1551.
DiZerega, G.S., DeCherney, A.H., Diamond, M.P., Dunn, R.C., Goldberg, E.P., Haney, A.F., et al., 1997. Pelvic Surgery: Adhesion Formation and Prevention. Springer.
Doostdar, H., Duthie, S.J., Burke, M.D., Melvin, W.T., Grant, M.H., 1988. The influence of culture medium composition on drug metabolising enzyme activities of the human liver derived hep G2 cell line. FEBS Lett. 241 (1–2), 15–18.
Duryee, M.J., Willis, M.S., Schaffert, C.S., Reidelberger, R.D., Dusad, A.A., Klassen, D.R., et al., 2014. Precision-cut liver slices from diet-induced obese rats exposed to ethanol are susceptible to oxidative stress and increased fatty acid synthesis. Am. J. Physiol. Gastrointest. Liver Physiol. 306 (3), G208–G217.
Elaut, G., Vanhaecke, T., Heyden, Y.V., Rogiers, V., 2005. Spontaneous apoptosis, necrosis, energy status, glutathione levels and biotransformation capacities of isolated rat hepatocytes in suspension: effect of the incubation medium. Biochem. Pharmacol. 69 (12), 1829–1838.
Elferink, M.G.L., Olinga, P., Draaisma, A.L., Merema, M.T., Bauerschmidt, S., Polman, J., et al., 2008. Microarray analysis in rat liver slices correctly predicts in vivo hepatotoxicity. Toxicol. Appl. Pharmacol. 229 (3), 300–309.
Friedl, P., 2009. Collective cell migration in morphogenesis, regeneration and cancer. Nat. Rev. Mol. Cell Biol. 10 (7), 445–457.
Geimer, P., 1991. The epidermal growth factor-induced migration of rat liver epithelial cells is associated with a transient inhibition of DNA synthesis. J. Cell Sci. 100, 349–355.
Goethals, F., Deboyser, D., Lefebvre, V., De Coster, I., Roberfroid, M., 1990. Adult rat liver slices as a model for studying the hepatotoxicity of vincaalkaloids. Toxicol. in Vitro 4 (4–5), 435–438.
Groothuis, G.M.M., Casini, A., Meurs, H., Olinga, P., 2014. Translational research in pharmacology and toxicology using precision-cut tissue slices. In: Coleman, R. (Ed.), Human-Based Systems for Translational Research, 1st ed. Royal Society of Chemistry., pp. 27–38.
Guyot, C., 2007a. Fibrogenic cell fate during fibrotic tissue remodelling observed in rat and human cultured liver slices. J. Hepatol. 46 (1), 142–150.
Guyot, C., 2007b. Specific activation of the different fibrogenic cells in rat cultured liver slices mimicking in vivo situations. Virchows Arch. 450 (5), 503–512.
Hadi, M., Chen, Y., Starokozhko, V., Merema, M.T., Groothuis, G.M.M., 2012. Mouse precision-cut liver slices as an ex vivo model to study idiosyncratic drug-induced liver injury. Chem. Res. Toxicol. 25 (9), 1938–1947.
Halliwell, B., 2014. Cell culture, oxidative stress, and antioxidants: avoiding pitfalls. Biomed. J. 37 (3), 99–105.
Hashemi, E., Till, C., Ioannides, C., 1999. Stability of phase II conjugation systems in cultured precision-cut rat hepatic slices. Toxicol. in Vitro 13 (3), 459–466.
Ijzer, J., 2006. Morphological characterisation of portal myofibroblasts and hepatic stellate cells in the normal dog liver. Comp. Hepatol. 5.
Ilina, O., 2009. Mechanisms of collective cell migration at a glance. J. Cell Sci. 122 (Pt), 3203–3208.
Iyer, V.V., Yang, H., Ierapetritou, M.G., Roth, C.M., 2010. Effects of glucose and insulin on HepG2-C3A cell metabolism. Biotechnol. Bioeng. 107 (2), 347–356.
Jetten, M.J.A., Claessen, S.M., Dejong, C.H.C., Lahoz, A., Castell, J.V., van Delft, J.H.M., et al., 2014. Interindividual variation in response to xenobiotic exposure established in precision-cut human liver slices. Toxicology 323 (0), 61–69.
Kara, B., Daglioglu, K., Doran, F., Akkiz, H., Sandikci, M., Kara, I.O., 2009. Expression of mesenchymal, hematopoietic, and biliary cell markers in adult rat hepatocytes after partial hepatectomy. Transplant. Proc. 41 (10), 4401–4404.
Kinkel, A., Fernyhough, M., Helterline, D., Vierck, J., Oberg, K., Vance, T., et al., 2004. Oil red-O stains non-adipogenic cells: a precautionary note. Cytotechnology 46 (1), 49–56.
Kostadinova, R., Boess, F., Applegate, D., Suter, L., Weiser, T., Singer, T., et al., 2013. A long-term three dimensional liver co-culture system for improved prediction of clinically relevant drug-induced hepatotoxicity. Toxicol. Appl. Pharmacol. 268 (1), 1–16.
Lange, J.R., Fabry, B., 2013. Cell and tissue mechanics in cell migration. Exp. Cell Res. 319 (16), 2418–2423.
Lerche-Langrand, C., Toutain, H.J., 2000. Precision-cut liver slices: characteristics and use for in vitro pharmaco-toxicology. Toxicology 153 (1–3), 221–253.
Lewis, W.H., 1923. Mesenchyme and mesothelium. J. Exp. Med. 38 (3), 257–262.
Li, Y., 2013. Mesothelial cells give rise to hepatic stellate cells and myofibroblasts via mesothelial-mesenchymal transition in liver injury. Proc. Natl. Acad. Sci. U. S. A. 110 (6), 2324–2329.
Lowry, O.H., Rosebrough, N.J., Farr, A.L., Randall, R.J., 1951. Protein measurement with the folin phenol reagent. J. Biol. Chem. 193 (1), 265–275.
Mallat, A., 2014. Autophagy: a multifaceted partner in liver fibrosis. Biomed. Res. Int. 2014.
Martignoni, M., 2006. Species differences between mouse, rat, dog, monkey and human CYP-mediated drug metabolism, inhibition and induction. Expert Opin. Drug Metab. Toxicol. 2 (6), 875–894.
Martin, H., 2002. Morphological and biochemical integrity of human liver slices in long-term culture: effects of oxygen tension. Cell Biol. Toxicol. 18 (2), 73–85.
Michelotti, G.A., Xie, G., Swiderska, M., Choi, S.S., Karaca, G., Krüger, L., et al., 2013. Smoothened is a master regulator of adult liver repair. J. Clin. Invest. 123 (6), 2380–2394.

Mutsaers, S.E., 2002. Mesothelial cells: their structure, function and role in serosal repair. Respirology 7 (3), 171–191.
Nassir, F., 2014. Role of mitochondria in nonalcoholic fatty liver disease. Int. J. Mol. Sci. 15 (5), 8713–8742.
Natarajan, A., Wagner, B., Sibilia, M., 2007. The EGF receptor is required for efficient liver regeneration. Proc. Natl. Acad. Sci. U. S. A. 104 (43), 17081–17086.
Nishioka, Y., 2008. Regeneration of peritoneal mesothelium in a rat model of peritoneal fibrosis. Ren. Fail. 30 (1), 97–105.
Oliveira, C.P., 2006. Liver mitochondrial dysfunction and oxidative stress in the pathogenesis of experimental nonalcoholic fatty liver disease. Braz. J. Med. Biol. Res. 39 (2), 189–194.
Parrish, A.R., Gandolfi, A.J., Brendel, K., 1995. Precision-cut tissue slices: applications in pharmacology and toxicology. Life Sci. 57 (21), 1887–1901.
Price, R.J., Ball, S.E., Renwick, A.B., Barton, P.T., Beamand, J.A., Lake, B.G., 1998. Use of precision-cut rat liver slices for studies of xenobiotic metabolism and toxicity: comparison of the krumdieck and brendel tissue slicers. Xenobiotica 28 (4), 361–371.
Roberts, R.A., Ganey, P.E., Ju, C., Kamendulis, L.M., Rusyn, I., Klaunig, J.E., 2007. Role of the kupffer cell in mediating hepatic toxicity and carcinogenesis. Toxicol. Sci. 96 (1), 2–15.
Rose, M.L., 2001. Transplant-Associated Coronary Artery Vasculopathy. Landes Bioscience.
Schaart, G., Hesselink, R., Keizer, H., van Kranenburg, G., Drost, M., Hesselink, M.C., 2004. A modified PAS stain combined with immunofluorescence for quantitative analyses of glycogen in muscle sections. Histochem. Cell Biol. 122 (2), 161–169.
Soldatow, V.Y., LeCluyse, E.L., Griffith, L.G., Rusyn, I., 2013. In vitro models for liver toxicity testing. Toxicol. Res. 2 (1), 23–39.
Song, Y., 2014. Autophagy in hepatic fibrosis. Biomed. Res. Int. 2014.
Sugimoto, R., 2005. High glucose stimulates hepatic stellate cells to proliferate and to produce collagen through free radical production and activation of mitogen-activated protein kinase. Liver Int. 25 (5), 1018–1026.
Suzuki, T., 2014. Hypoxia and fatty liver. World J. Gastroenterol. 20 (41), 15087–15097.
Toutain, H.J., Moronvalle-Halley, V., Sarsat, J.P., Chelin, C., Hoet, D., Leroy, D., 1998. Morphological and functional integrity of precision-cut rat liver slices in rotating organ culture and multiwell plate culture: effects of oxygen tension. Cell Biol. Toxicol. 14 (3), 175–190.
Valle, M.T., 1995. Antigen-presenting function of human peritoneum mesothelial cells. Clin. Exp. Immunol. 101 (1), 172–176.
van de Bovenkamp, M., Groothuis, G.M.M., Meijer, D.K.F., Olinga, P., 2008. Liver slices as a model to study fibrogenesis and test the effects of anti-fibrotic drugs on fibrogenic cells in human liver. Toxicol. in Vitro 22 (3), 771–778.
Vasilyev, A., Liu, Y., Mudumana, S., Mangos, S., Lam, P.Y., Majumdar, A., Zhao, J., Poon, K.L., Kondrychyn, I., Korzh, V., Drummond, I.A., 2009. Collective cell migration drives morphogenesis of the kidney nephron. PLoS Biol. 7 (1).
Vickers, A.E., 2006. Consequences of mitochondrial injury induced by pharmaceutical fatty acid oxidation inhibitors is characterized in human and rat liver slices. Toxicol. in Vitro 20 (7), 1173–1182.
Vickers, A.E.M., Fisher, R.L., 2013. Evaluation of drug-induced injury and human response in precision-cut tissue slices. Xenobiotica 43 (1), 29–40.
Vickers, A.E.M., Saulnier, M., Cruz, E., Merema, M.T., Rose, K., Bentley, P., et al., 2004. Organ slice viability extended for pathway characterization: an in vitro model to investigate fibrosis. Toxicol. Sci. 82 (2), 534–544.
Wei, Y., 2008. Nonalcoholic fatty liver disease and mitochondrial dysfunction. World J. Gastroenterol. 14 (2), 193–199.
Westra, I.M., Oosterhuis, D., Groothuis, G.M.M., Olinga, P., 2014. Precision-cut liver slices as a model for the early onset of liver fibrosis to test antifibrotic drugs. Toxicol. Appl. Pharmacol. 274 (2), 328–338.
Xie, G., 2013. Evidence for and against epithelial-to-mesenchymal transition in the liver. Am. J. Physiol. Gastrointest. Liver Physiol. 305 (12), 881–890.
Yamamoto, H., Murawaki, Y., Kawasaki, H., 1995. Hepatic collagen synthesis and degradation during liver regeneration after partial hepatectomy. Hepatology 21 (1), 155–161.
Yang, L., 2008. Fate-mapping evidence that hepatic stellate cells are epithelial progenitors in adult mouse livers. Stem Cells 26 (8), 2104–2113.
Yoshioka, K., 2005. Cell proliferation activity of proliferating bile duct after bile duct ligation in rats. Vet. Pathol. 42 (3), 382–385.
Zhan, L., 2015. Hypoxia-inducible factor-1alpha in hepatic fibrosis: a promising therapeutic target. Biochimie 108C, 1–7.
Zhou, W., Zhang, Q., Qiao, L., 2014. Pathogenesis of liver cirrhosis. World J. Gastroenterol. 20 (23), 7312–7324.